Supplementary material for "Seasonal variation of tropospheric bromine monoxide over the Rann of Kutch salt marsh seen from space" by Hörmann et al.

C. Hörmann[1], H. Sihler[1,2], S. Beirle[1], M. J. M. Penning de Vries[1], U. Platt[2], and T. Wagner[1]

[1]Max-Planck-Institute for Chemistry, Mainz, Germany
[2]Institute for Environmental Physics, University of Heidelberg, Heidelberg, Germany

Correspondence to: C. Hörmann (c.hoermann@mpic.de)

1 Industrial salt evaporation complexes in the Rann of Kutch

Large industrial evaporation ponds are located near the coast of the *Great* and *Little Rann of Kutch* (see also Figure 2a, left in the main paper) and are used for the production of salt and the subsequent recovery of elemental bromine from sea bittern. Especially all over the *Little Rann*, the salt is also harvested from hand-built salt evaporation ponds that are constructed by thousands of local families year after year, after having been destroyed by the annually recurring monsoon flood.

A significant contribution of halogen emissions from the large artificial evaporation ponds that are used for salt/bromine mining can, however, be ruled out, as no trend can be seen from the measurements although the industrial facilities were massively

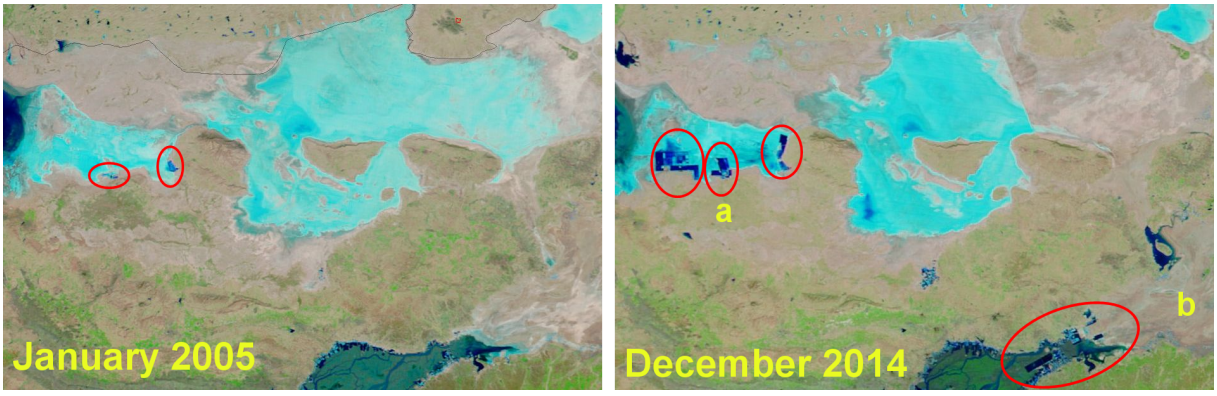

Figure 1. MODIS Band 7-2-1 observations over the Rann of Kutch area in January 2005 (left) and December (2014), indicating the massive extension of industrial salt mining complexes that can be identified by water inside the evaporation ponds appearing in dark blue (additionally marked by red circles). Landsat images from Google Earth© for regions **a** and **b** can be found in Figs. 2 and 3.

expanded after 2009. Figure 1 shows MODIS Band 7-2-1 images for the *Rann of Kutch* area in January 2005 and December 2014. The artificial evaporation ponds, marked by red circles, can be identified by water that appears in dark blue in contrast to the bright salty surface that appears light blue. A direct comparison of both panels clearly shows that the number and extent of the industrial salt mining complexes increased strongly during the time frame of the analyzed OMI data set. Most of the additional facilities that show up in Figure 1 (right) were built in 2009/2010. A closer look to such evaporation ponds is given in Figs. 2 and 3, where Landsat images from Google Earth© are shown for the regions indicated by **a** and **b** in Figure 1 (right).

Figure 2. Landsat images from Google Earth© indicating the large industrial salt/bromine mining complexes including evaporation ponds at the western part of the Great Rann of Kutch. The right panel shows a zoomed version of the facility that is marked by the yellow rectangle of the left panel. The major part of the evaporation ponds were built in 2009/2010.

Figure 3. Landsat images from Google Earth© indicating hand-built salt evaporation ponds all over the Little Rann of Kutch that are constructed by thousands of local families year after year. The right panel shows a zoomed version of the facility that is marked by the yellow rectangle of the left panel. All evaporation ponds are rebuilt after having been destroyed by the annually recurring monsoon flood.

2 OMI BrO VCDs 2004–2014

This section includes all monthly mean BrO VCD maps for the Rann of Kutch salt marsh to illustrate the annual variations and the seasonal cycle. For further details please also see Section 4 of the main paper.

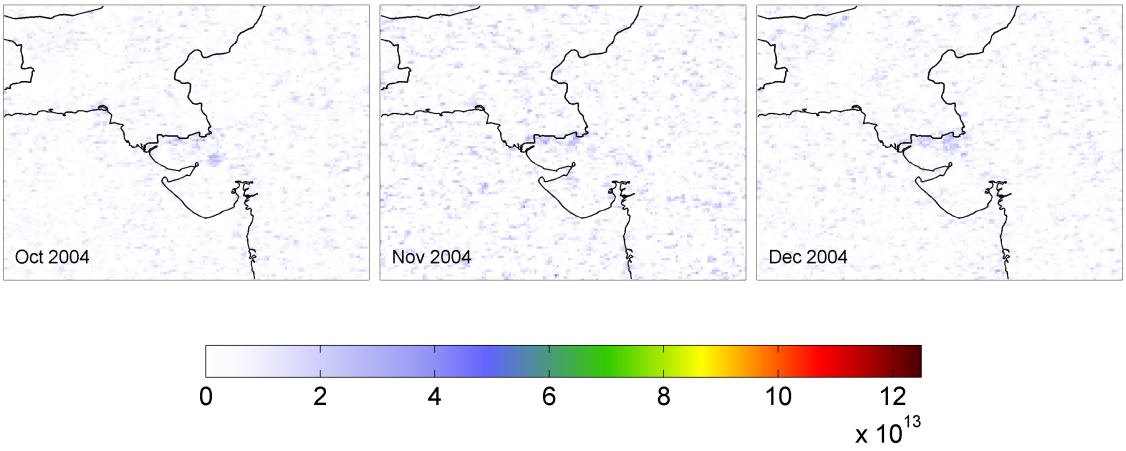

Figure 4. Seasonal variation of monthly mean BrO VCD over the Rann of Kutch as seen by OMI during 2004. Please note that OMI data is only available since October 2004.

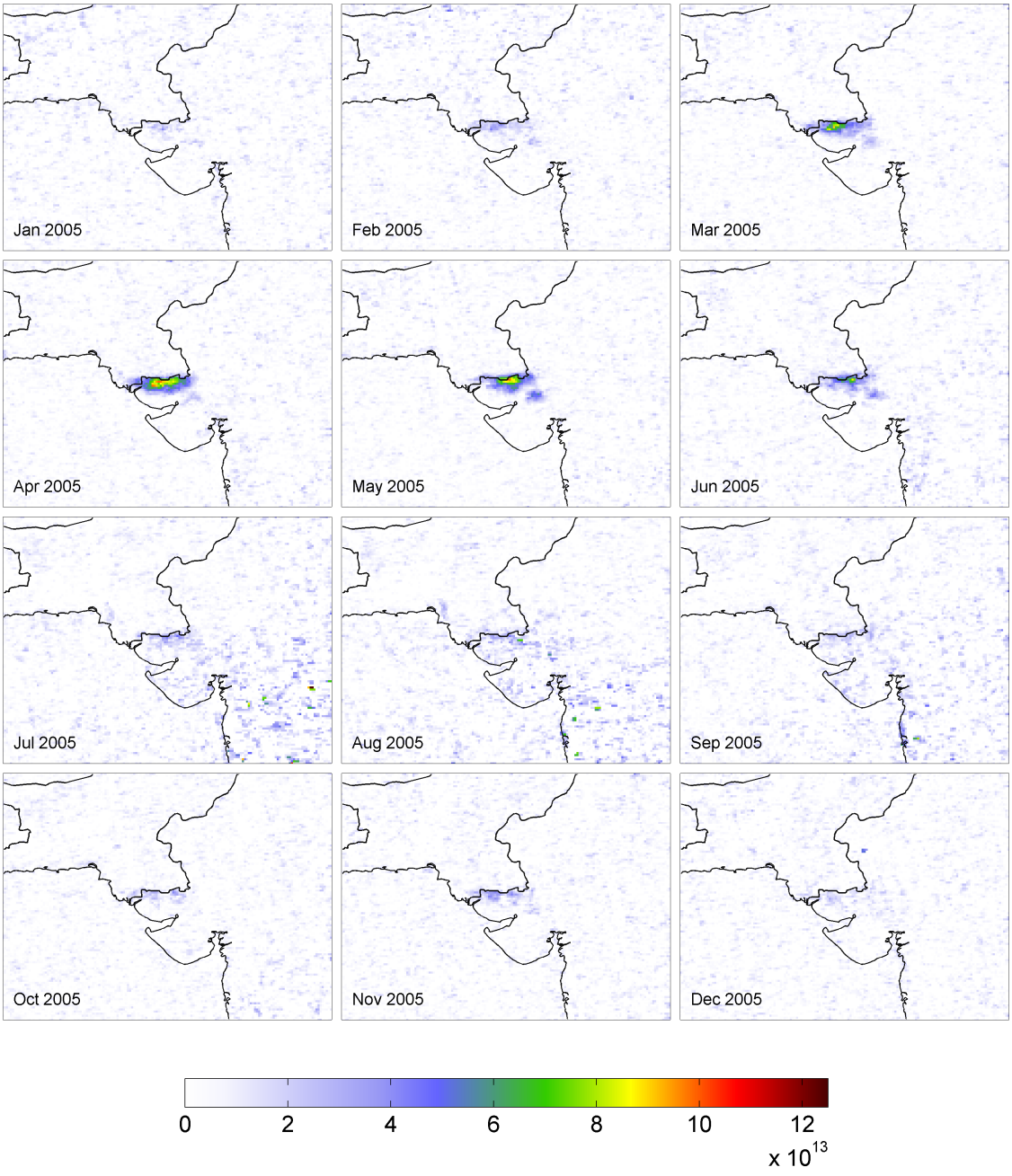

Figure 5. Seasonal variation of monthly mean BrO VCD over the Rann of Kutch as seen by OMI during 2005.

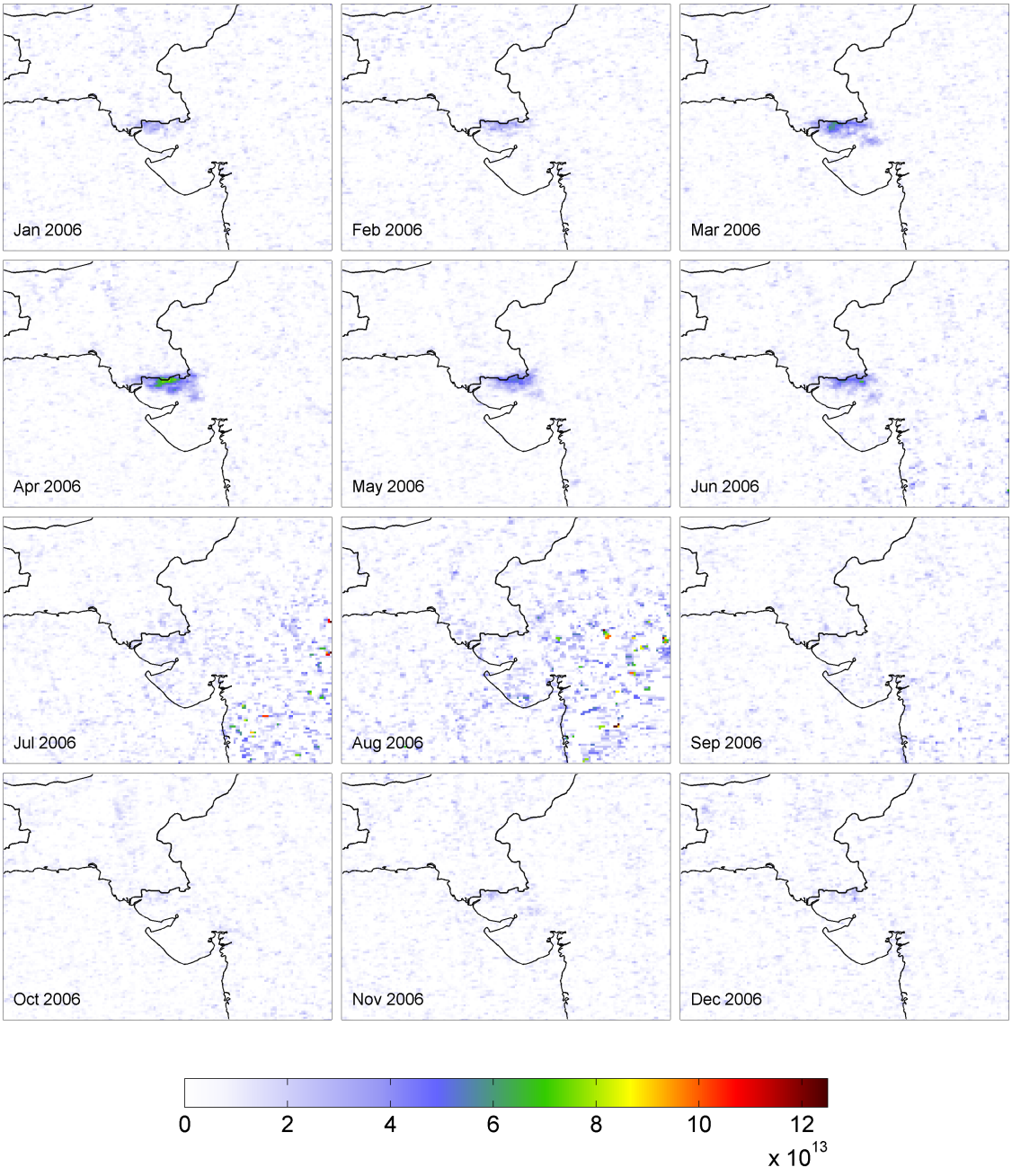

Figure 6. Seasonal variation of monthly mean BrO VCD over the Rann of Kutch as seen by OMI during 2006.

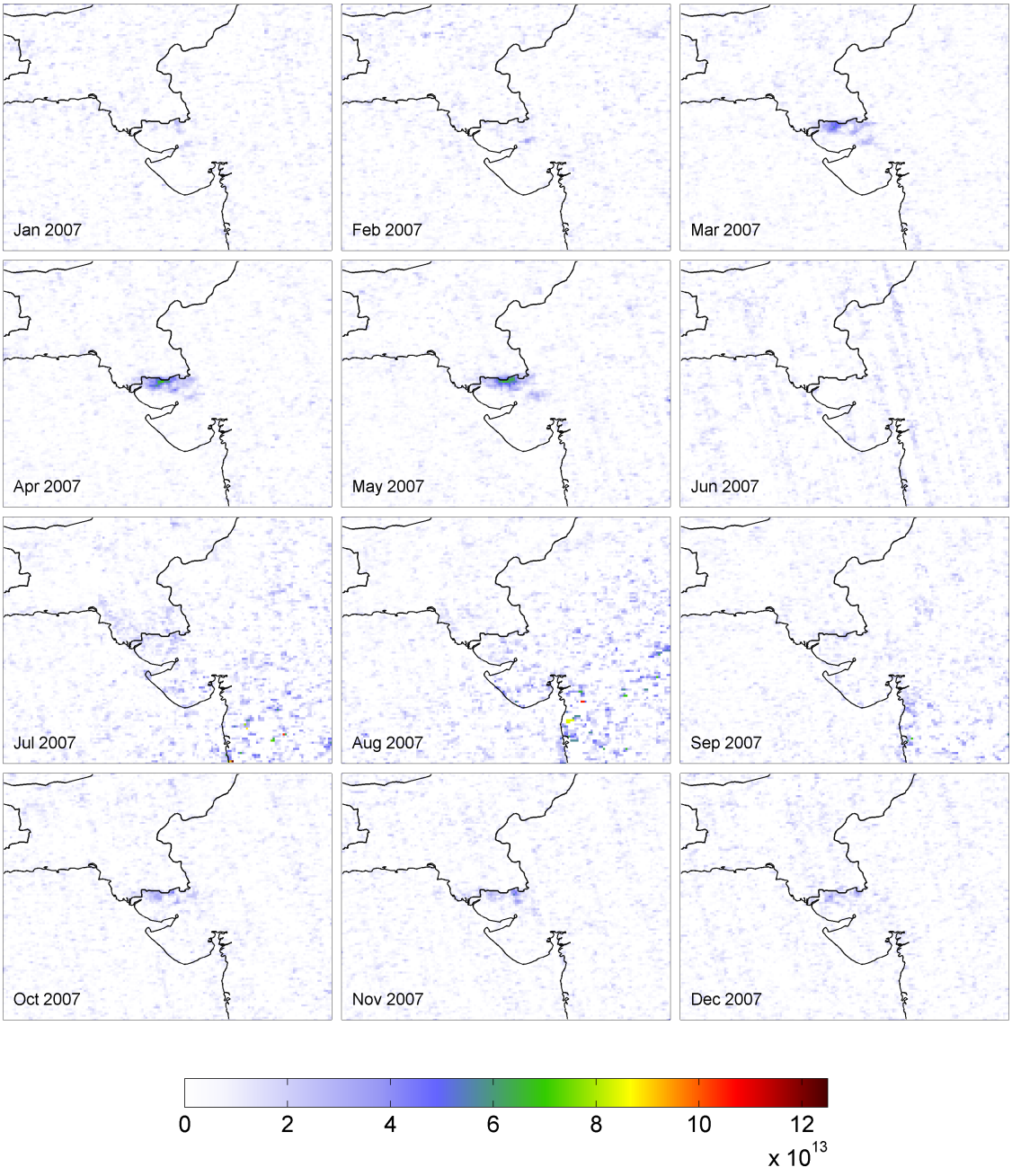

Figure 7. Seasonal variation of monthly mean BrO VCD over the Rann of Kutch as seen by OMI during 2007.

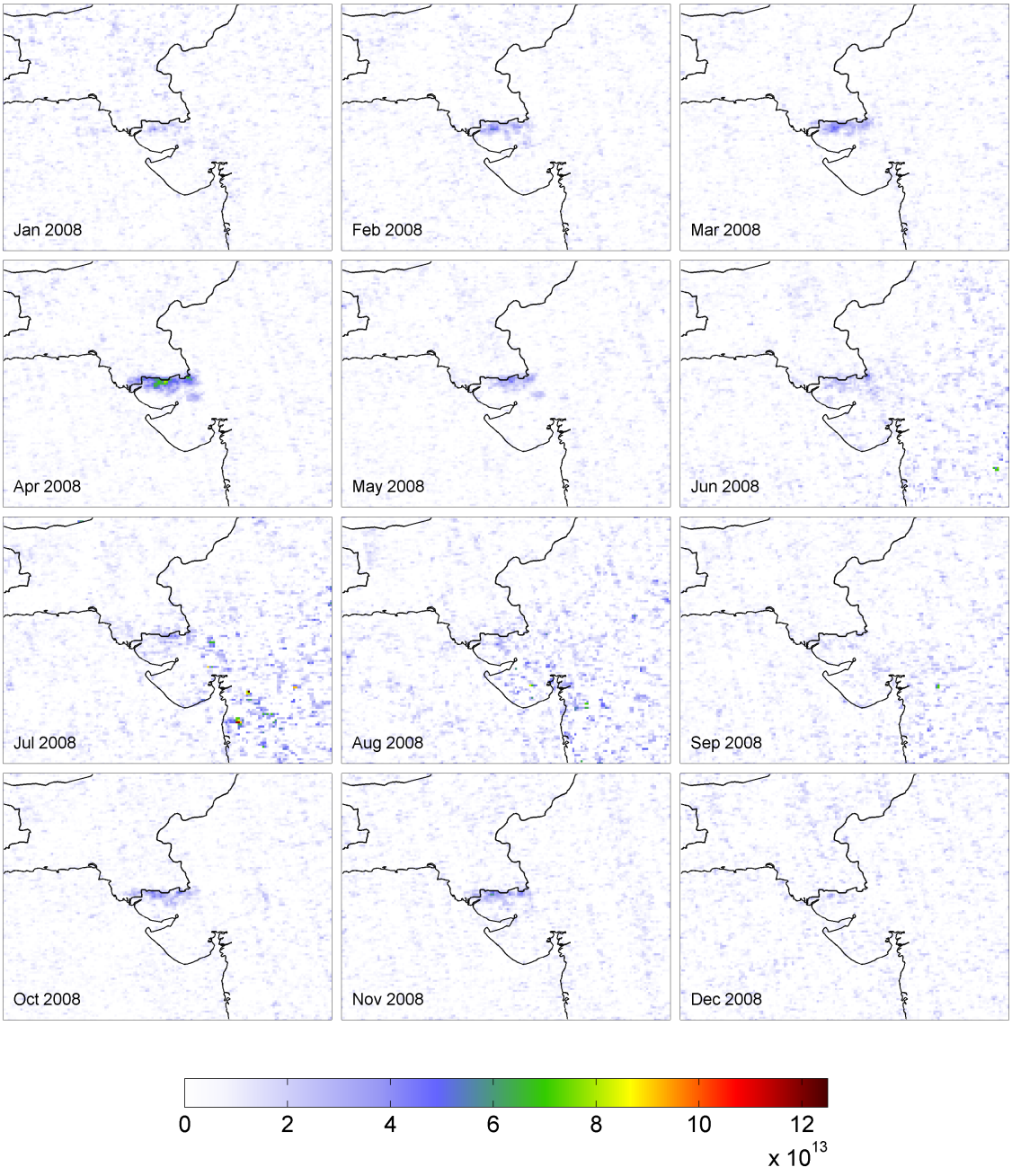

Figure 8. Seasonal variation of monthly mean BrO VCD over the Rann of Kutch as seen by OMI during 2008.

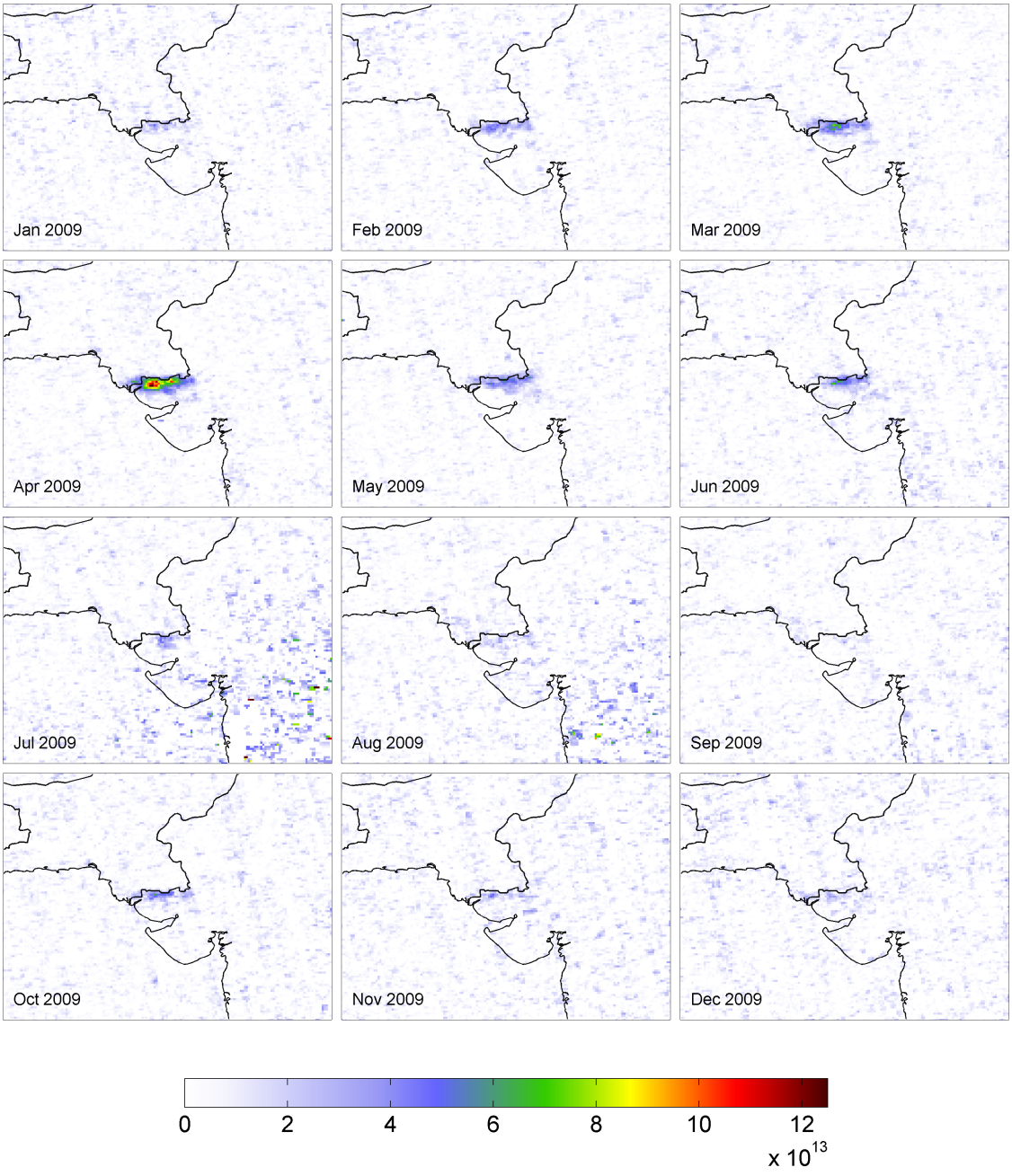

Figure 9. Seasonal variation of monthly mean BrO VCD over the Rann of Kutch as seen by OMI during 2009.

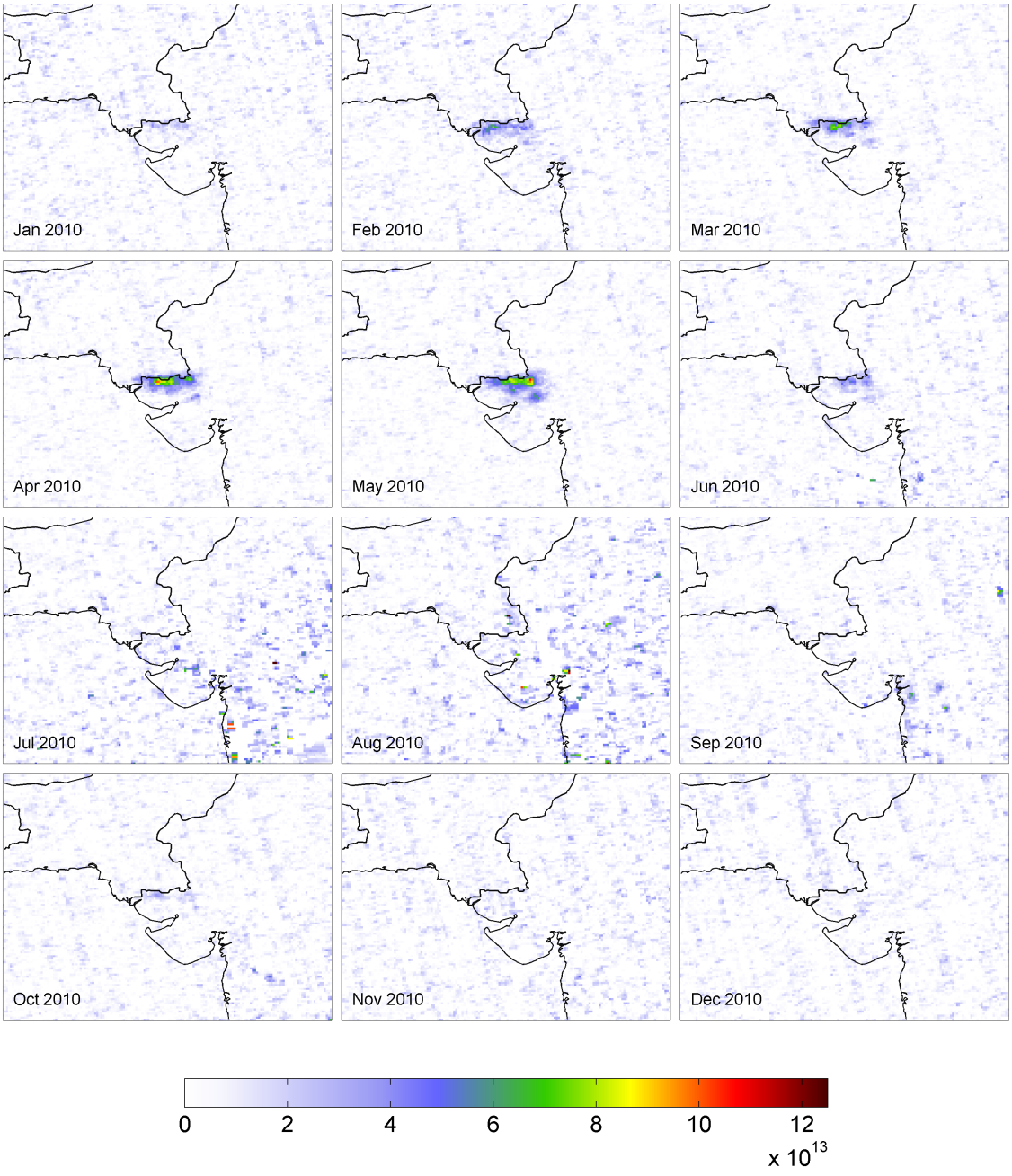

Figure 10. Seasonal variation of monthly mean BrO VCD over the Rann of Kutch as seen by OMI during 2010.

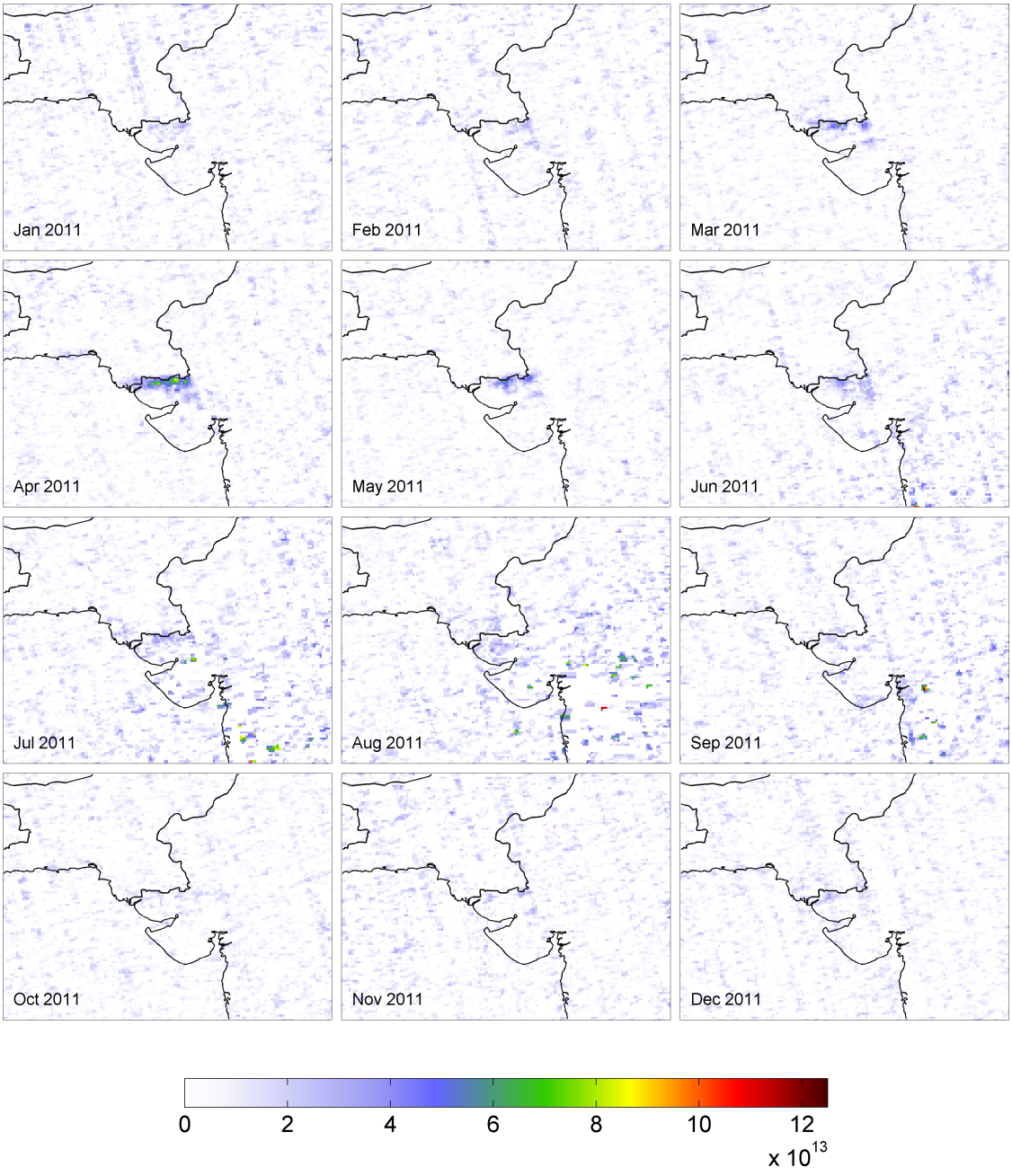

Figure 11. Seasonal variation of monthly mean BrO VCD over the Rann of Kutch as seen by OMI during 2011.

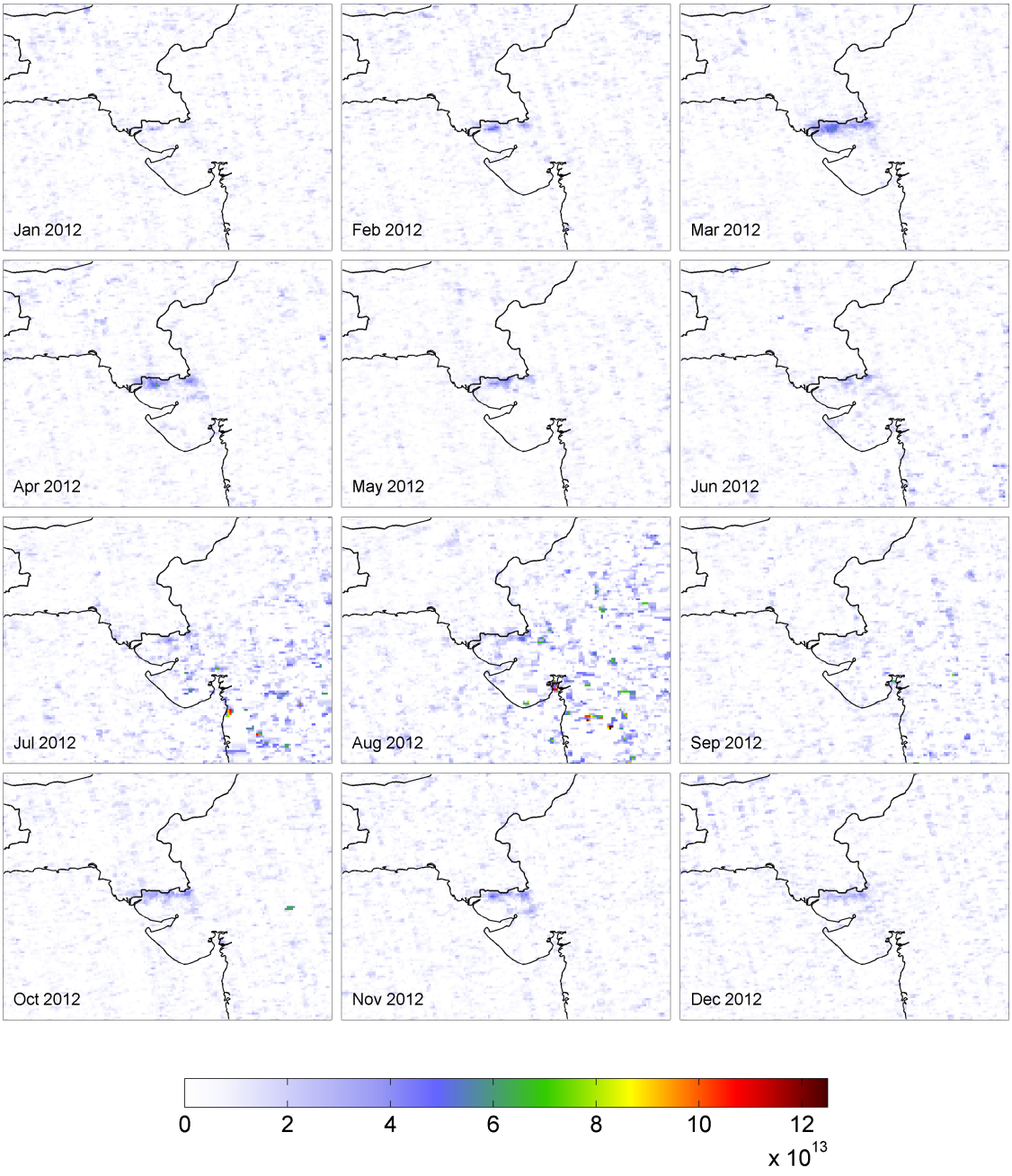

Figure 12. Seasonal variation of monthly mean BrO VCD over the Rann of Kutch as seen by OMI during 2012.

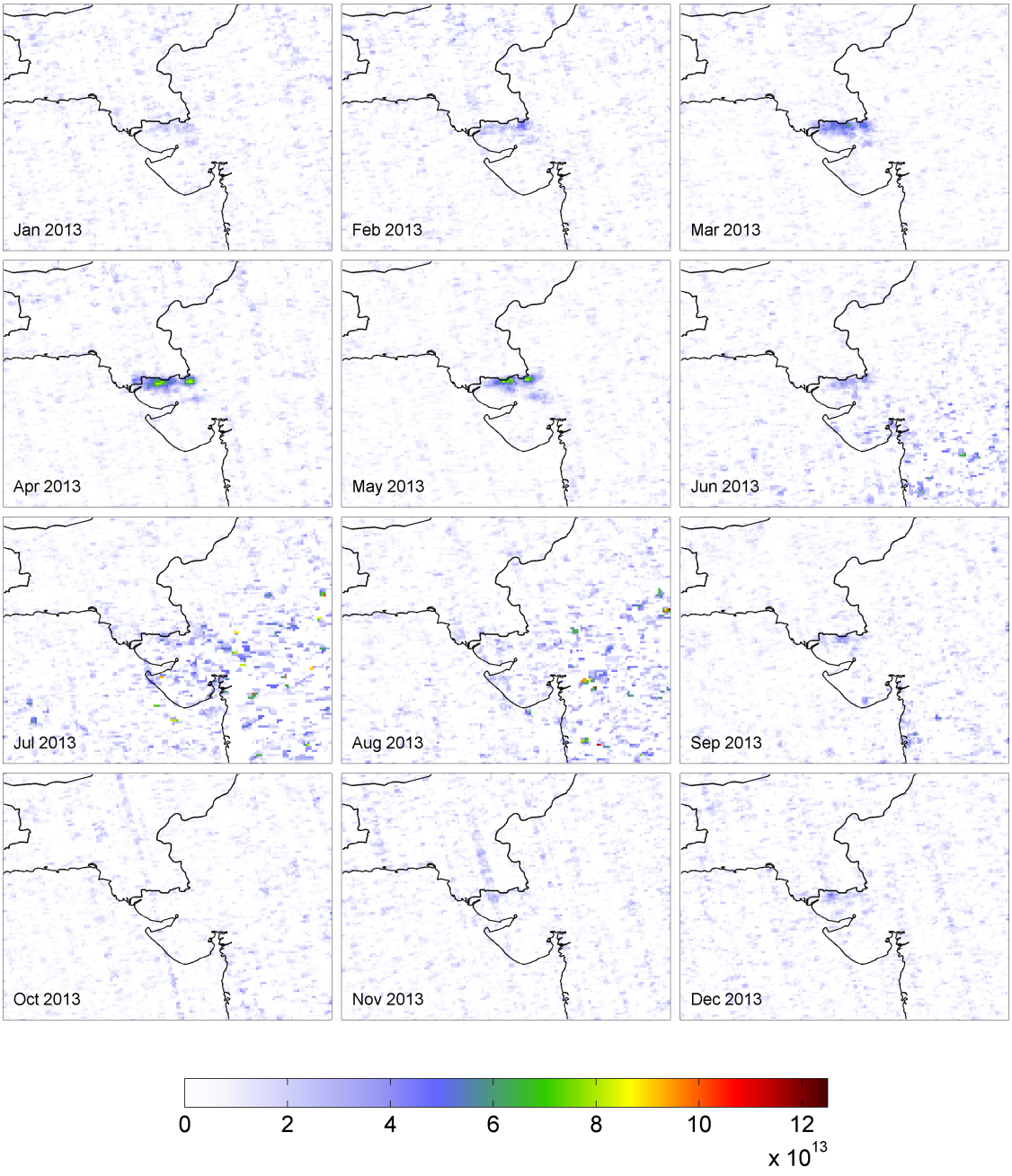

Figure 13. Seasonal variation of monthly mean BrO VCD over the Rann of Kutch as seen by OMI during 2013.

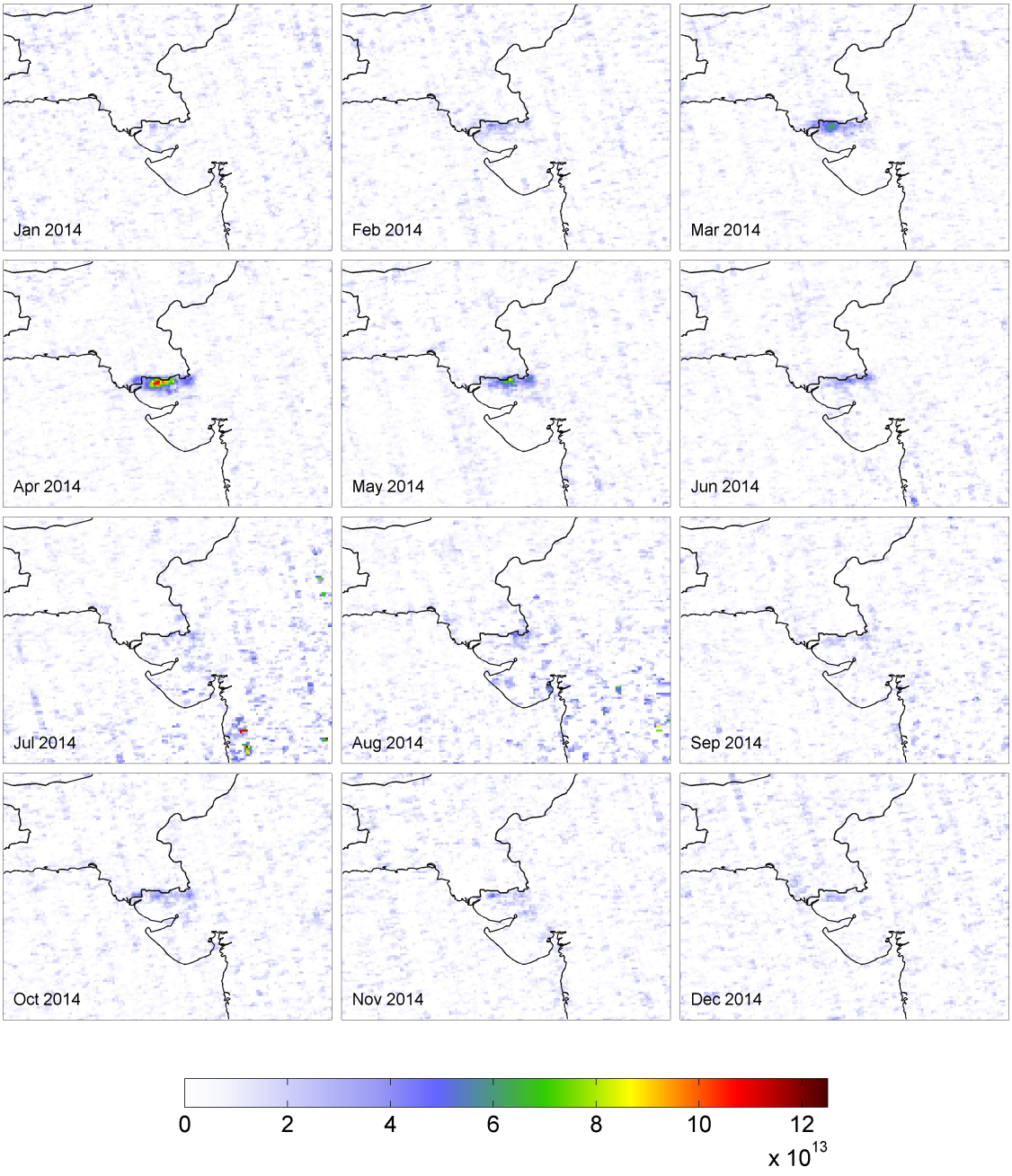

Figure 14. Seasonal variation of monthly mean BrO VCD over the Rann of Kutch as seen by OMI during 2014.

3 OMI Reflectivity at 331 nm 2004–2014

This section includes all OMI monthly mean maps of the reflectivity at 331 nm over the Rann of Kutch salt marsh to illustrate the annual variations. For further details please also see Section 4.1 of the main paper.

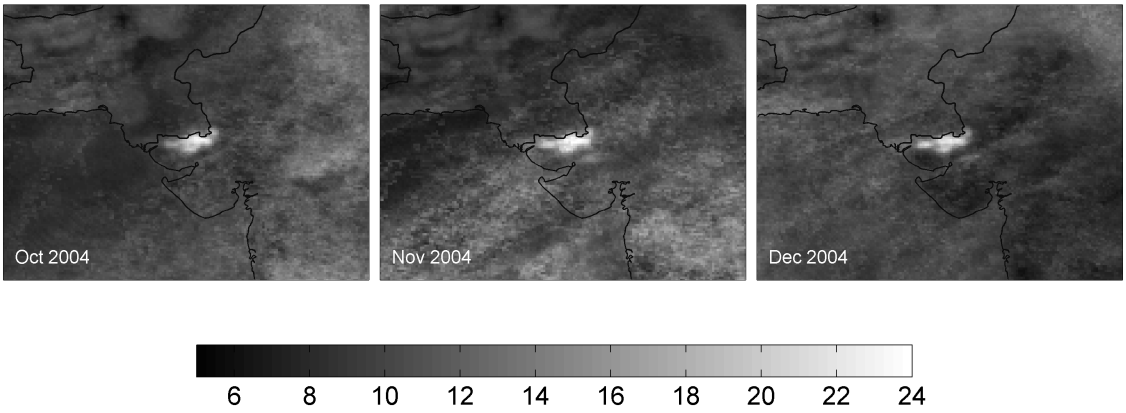

Figure 15. Seasonal variation of the monthly mean reflectivity at 331 nm over the Rann of Kutch as seen by OMI during 2004 (same data selection as in Figure 4, i.e. for CF<0.3). Please note that OMI data is only available since October 2004.

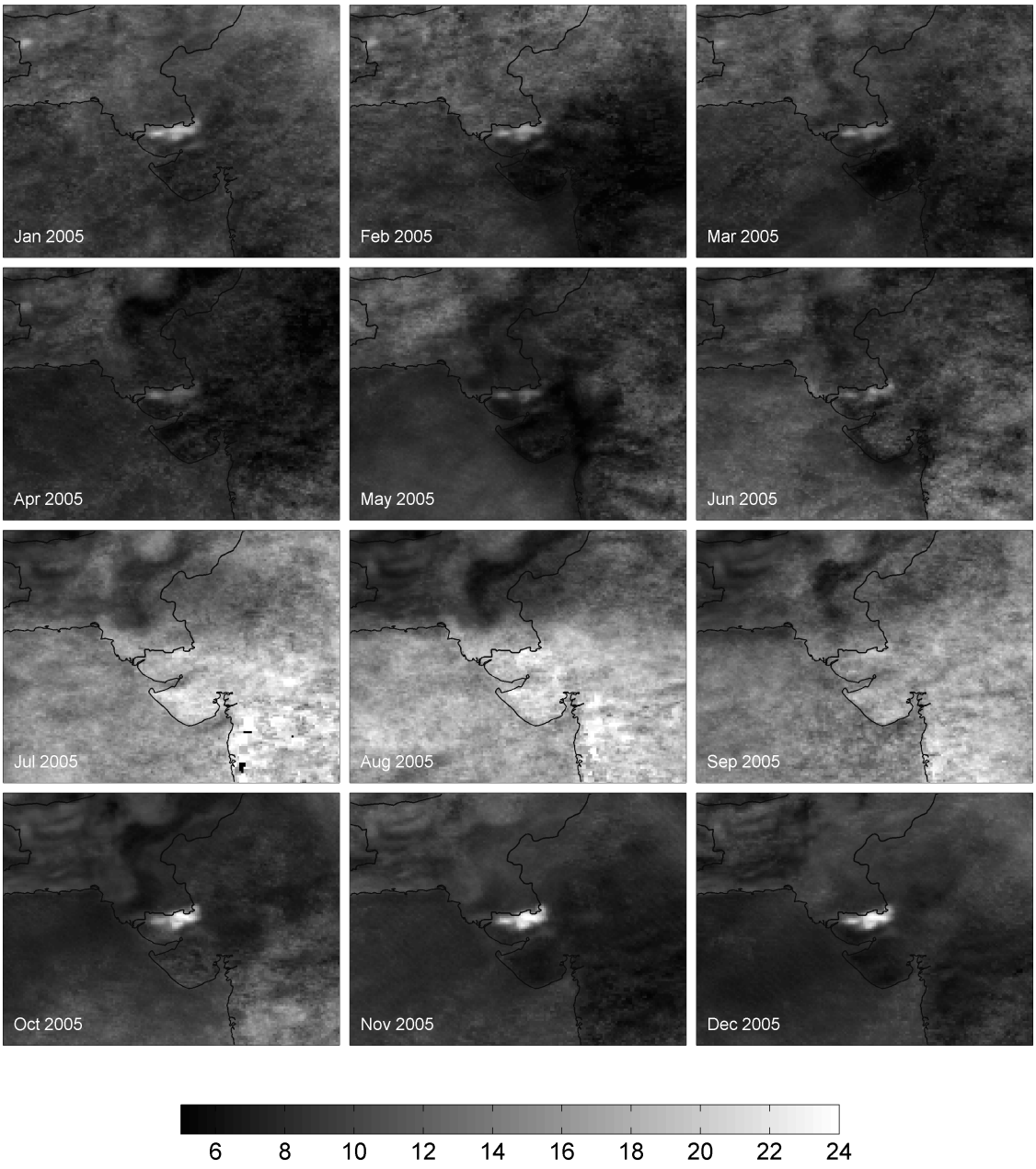

Figure 16. Seasonal variation of the monthly mean reflectivity at 331 nm over the Rann of Kutch as seen by OMI during 2005 (same data selection as in Figure 5, i.e. for CF<0.3).

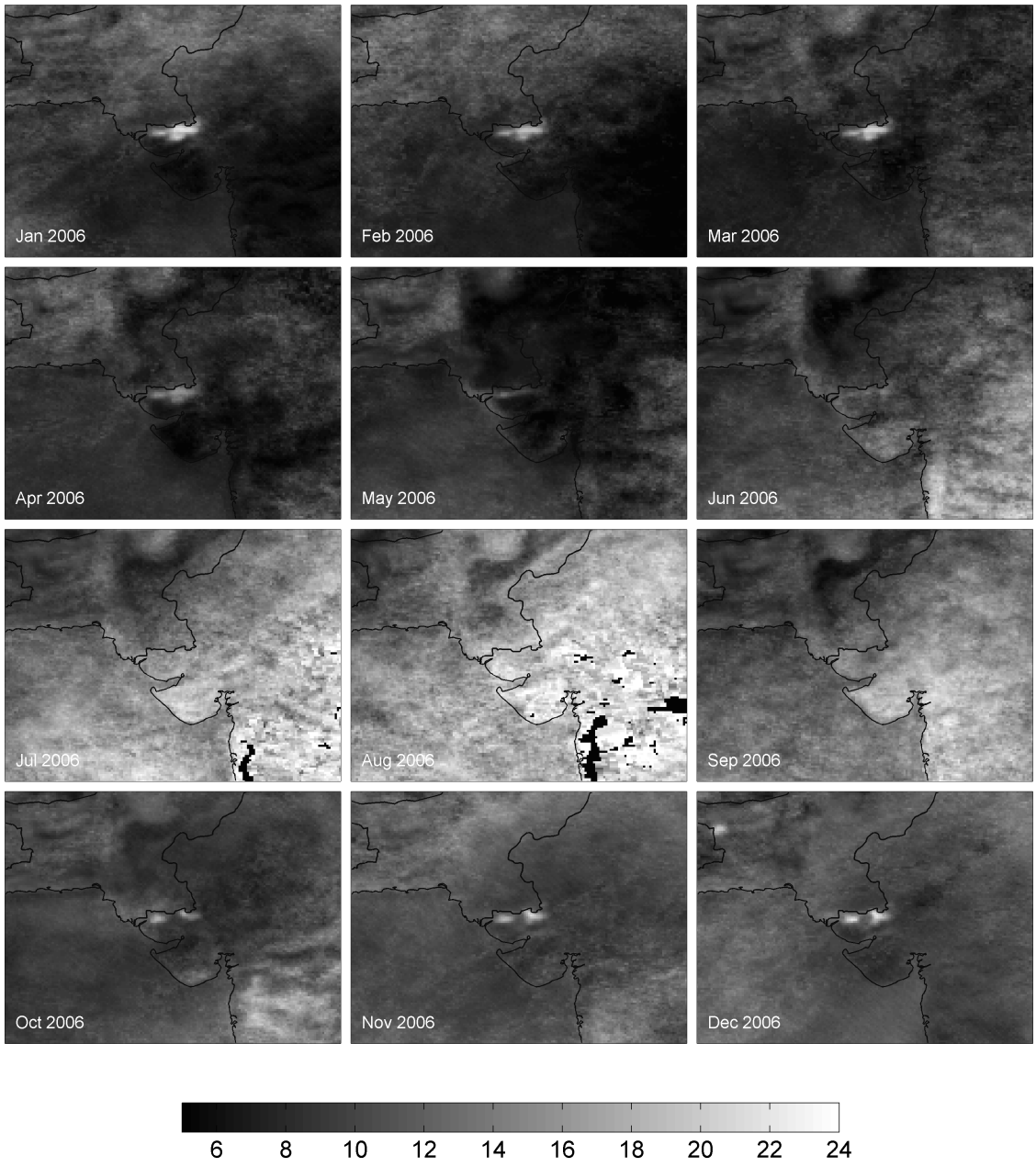

Figure 17. Seasonal variation of the monthly mean reflectivity at 331 nm over the Rann of Kutch as seen by OMI during 2006 (same data selection as in Figure 6, i.e. for CF<0.3).

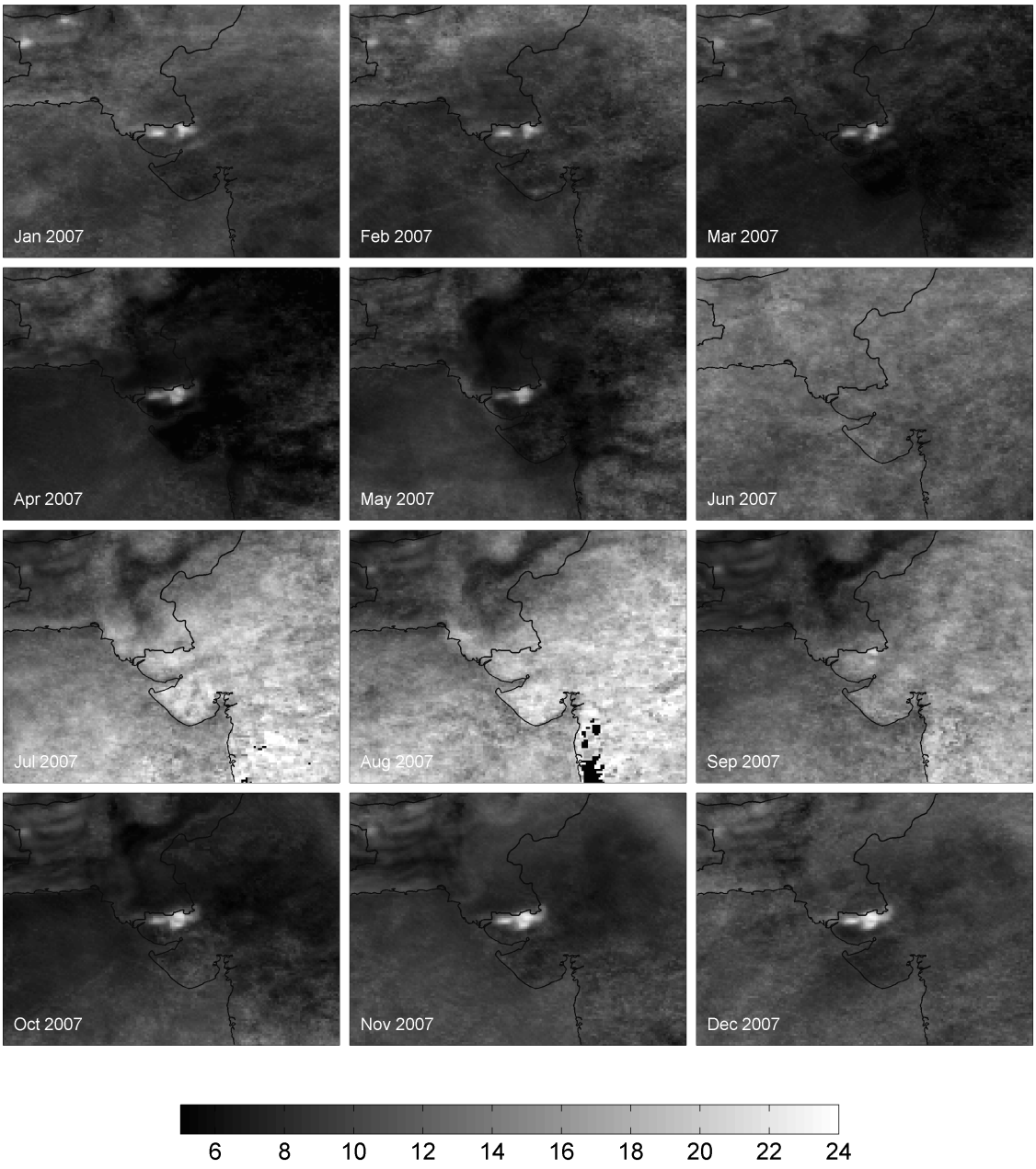

Figure 18. Seasonal variation of the monthly mean reflectivity at 331 nm over the Rann of Kutch as seen by OMI during 2007 (same data selection as in Figure 7, i.e. for CF<0.3).

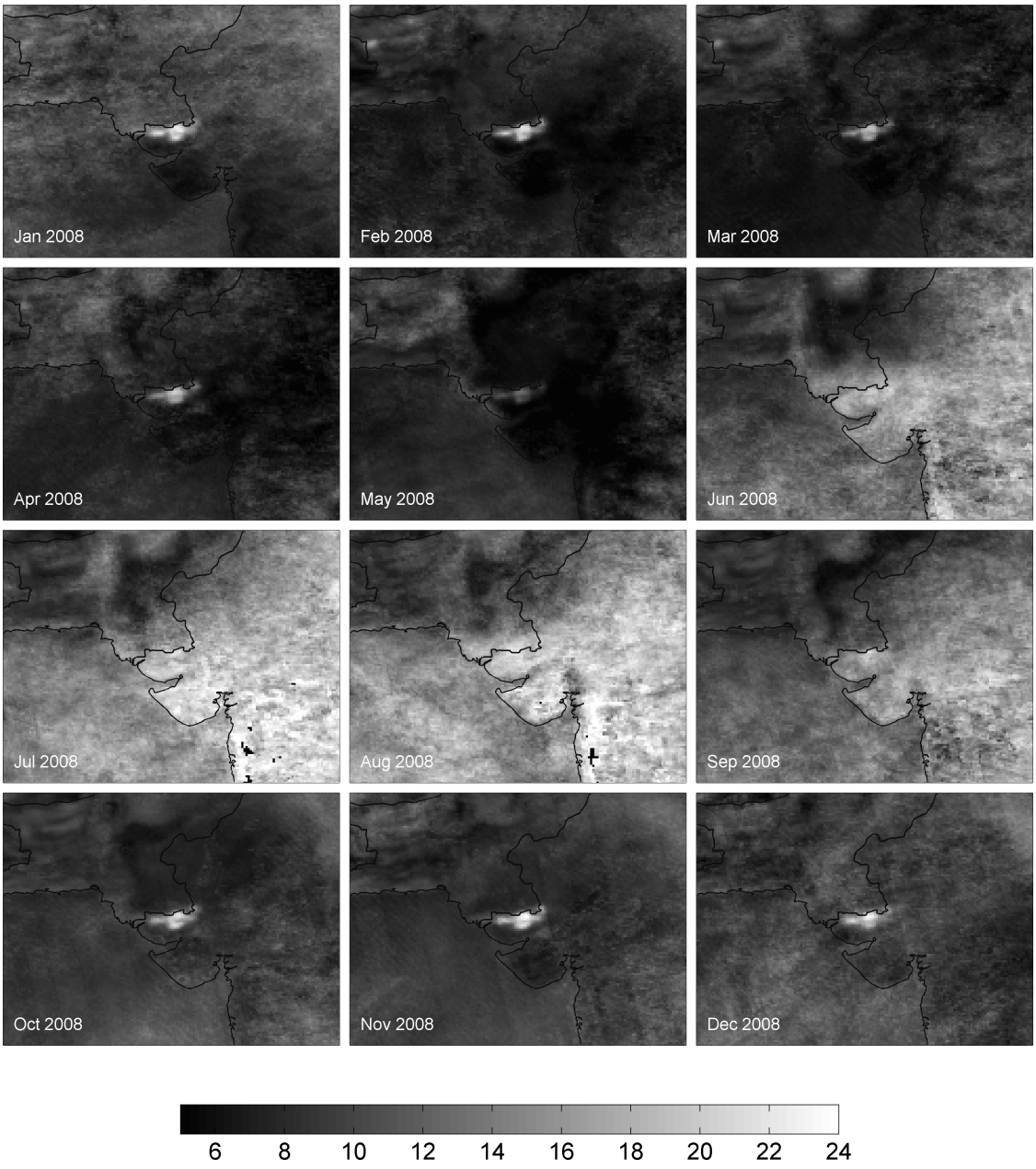

Figure 19. Seasonal variation of the monthly mean reflectivity at 331 nm over the Rann of Kutch as seen by OMI during 2008 (same data selection as in Figure 8, i.e. for CF<0.3).

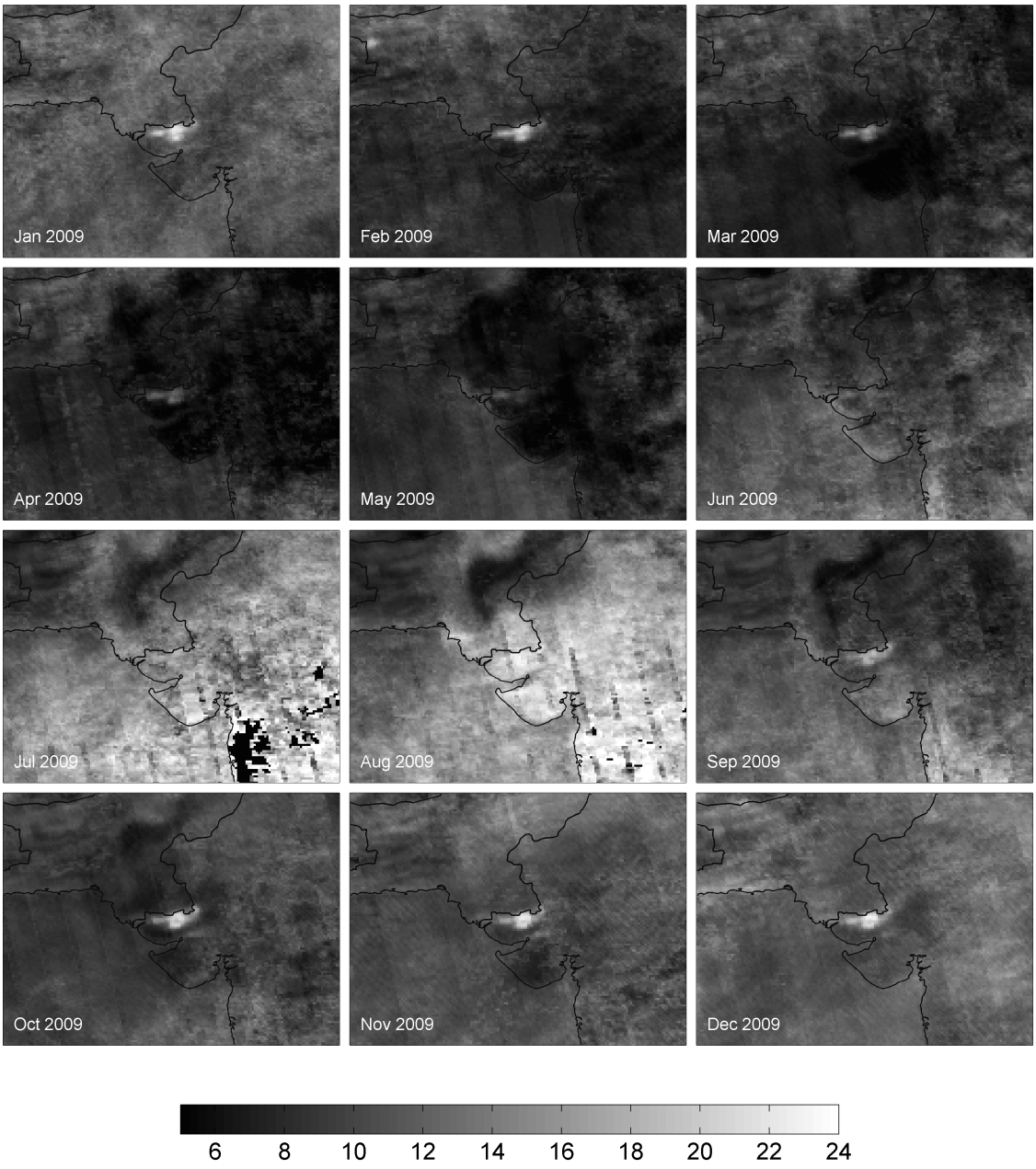

Figure 20. Seasonal variation of the monthly mean reflectivity at 331 nm over the Rann of Kutch as seen by OMI during 2009 (same data selection as in Figure 9, i.e. for CF<0.3).

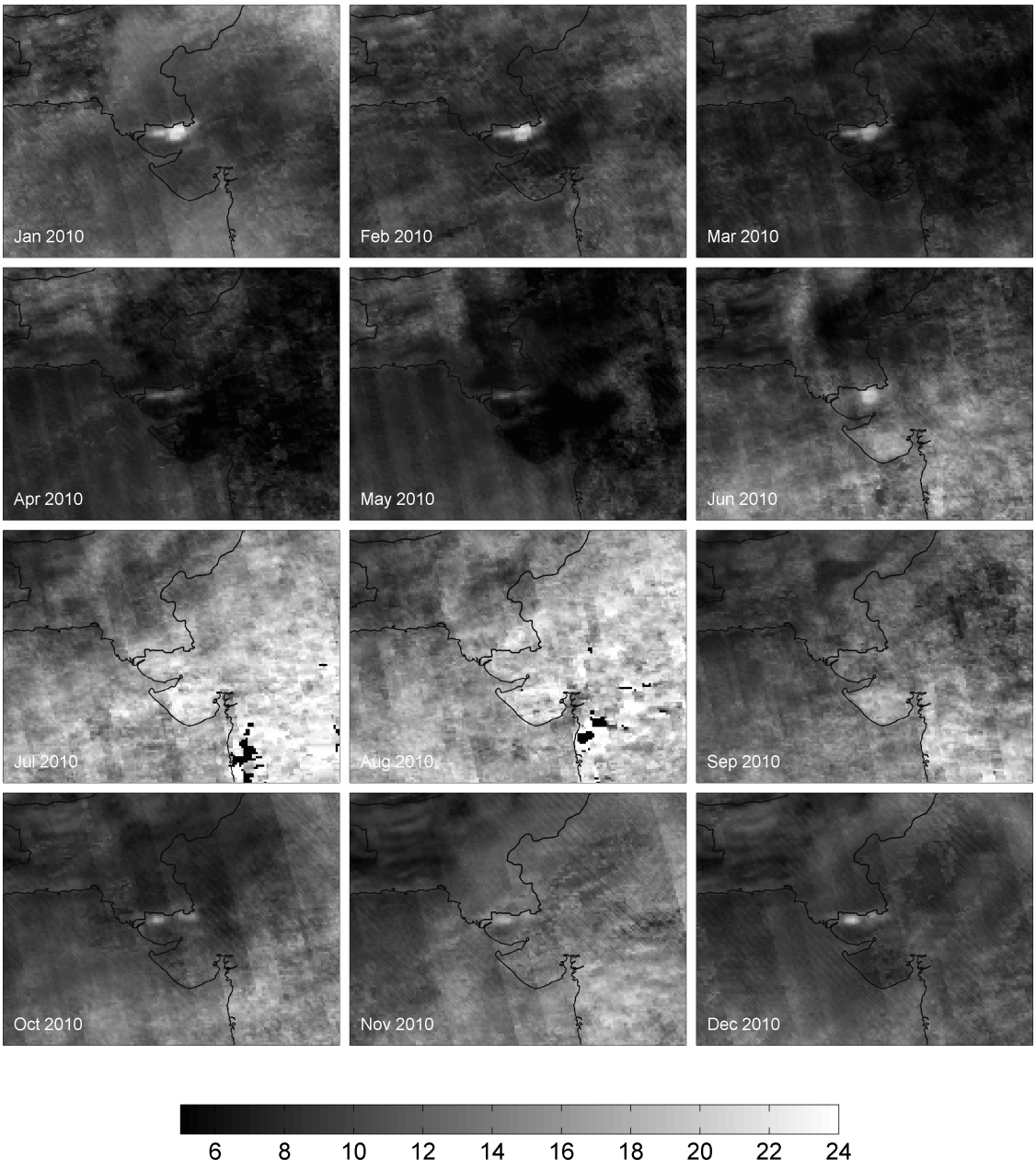

Figure 21. Seasonal variation of the monthly mean reflectivity at 331 nm over the Rann of Kutch as seen by OMI during 2010 (same data selection as in Figure 10, i.e. for CF<0.3).

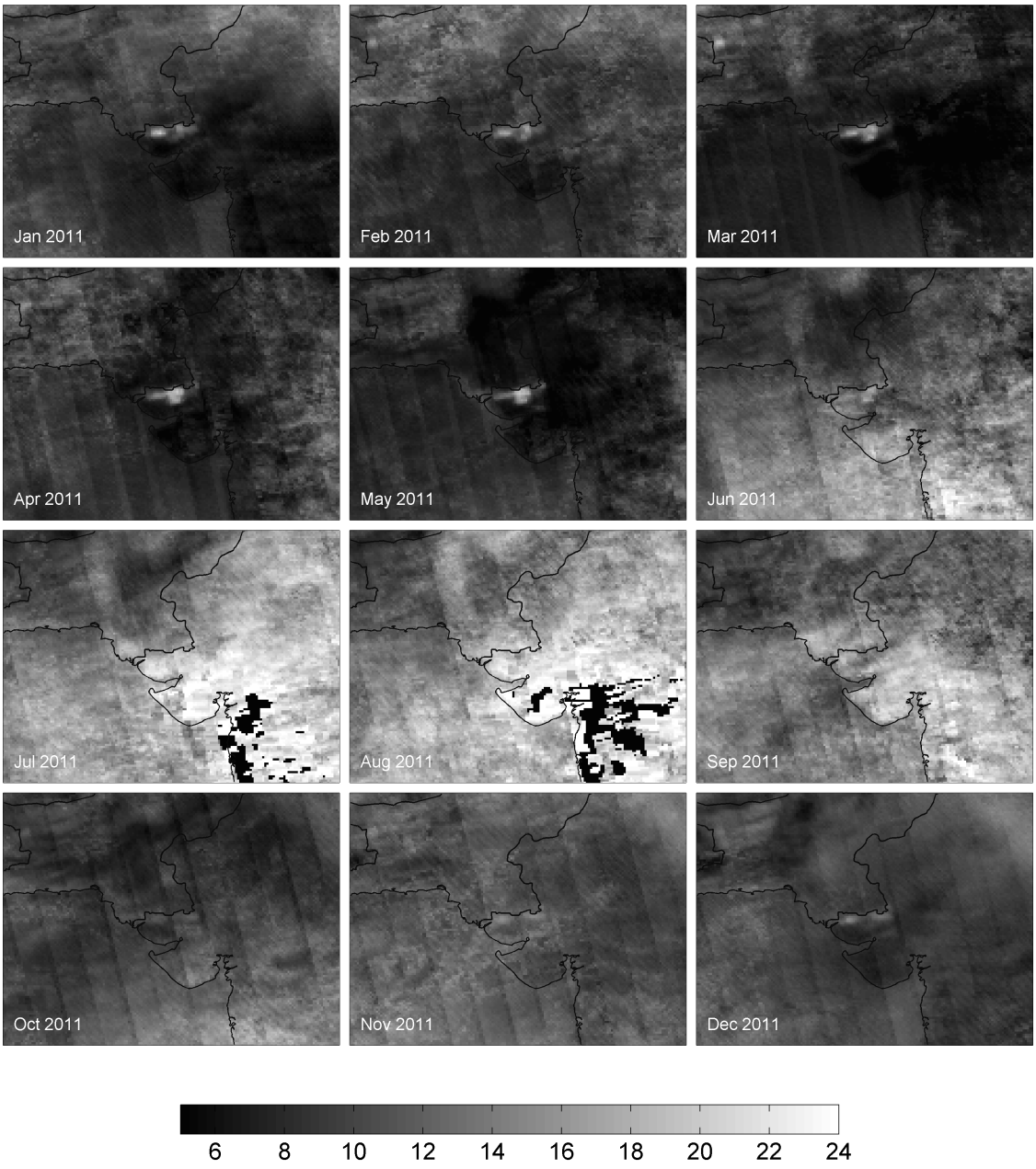

Figure 22. Seasonal variation of the monthly mean reflectivity at 331 nm over the Rann of Kutch as seen by OMI during 2011 (same data selection as in Figure 11, i.e. for CF<0.3).

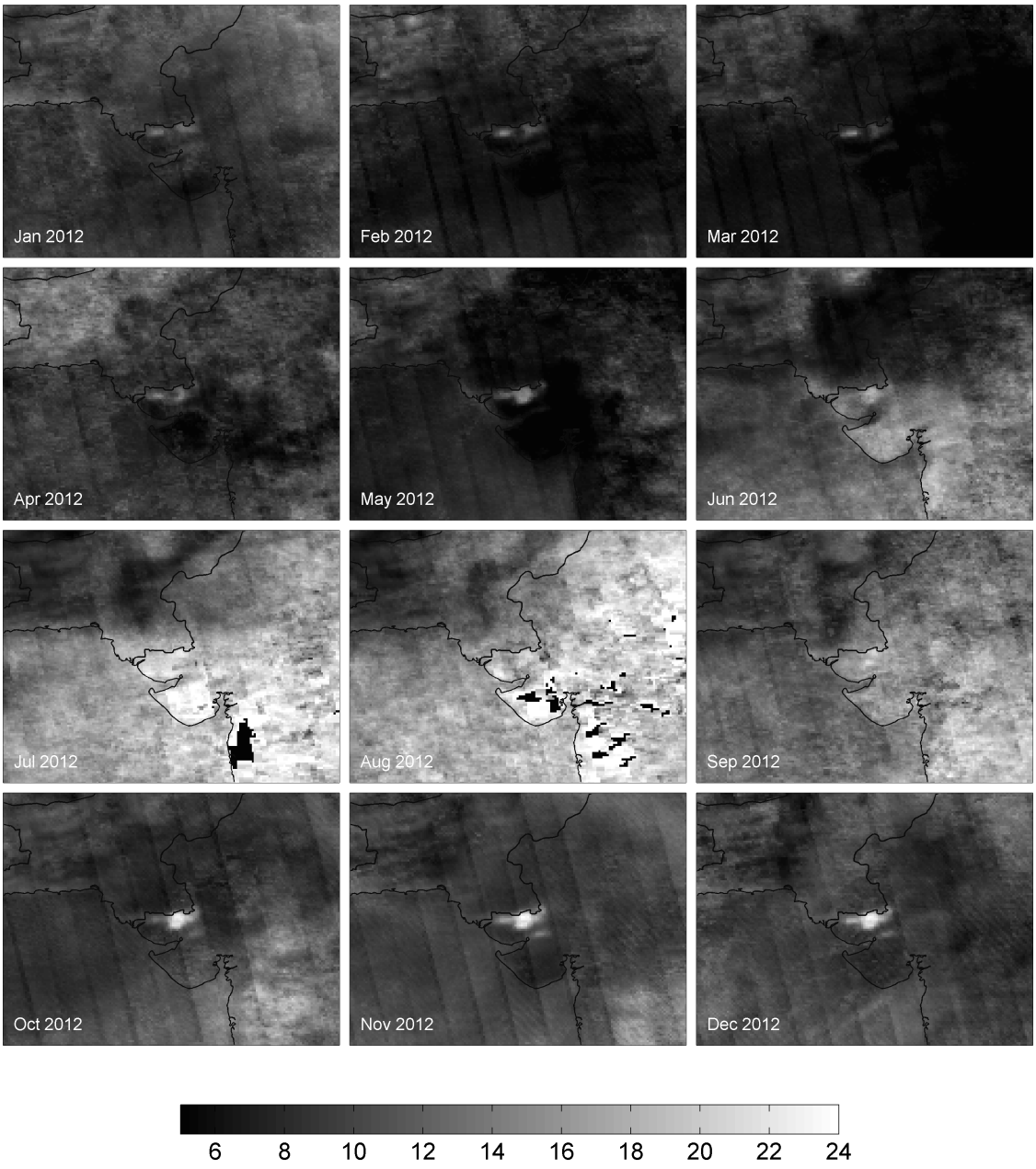

Figure 23. Seasonal variation of the monthly mean reflectivity at 331 nm over the Rann of Kutch as seen by OMI during 2012 (same data selection as in Figure 12, i.e. for CF<0.3).

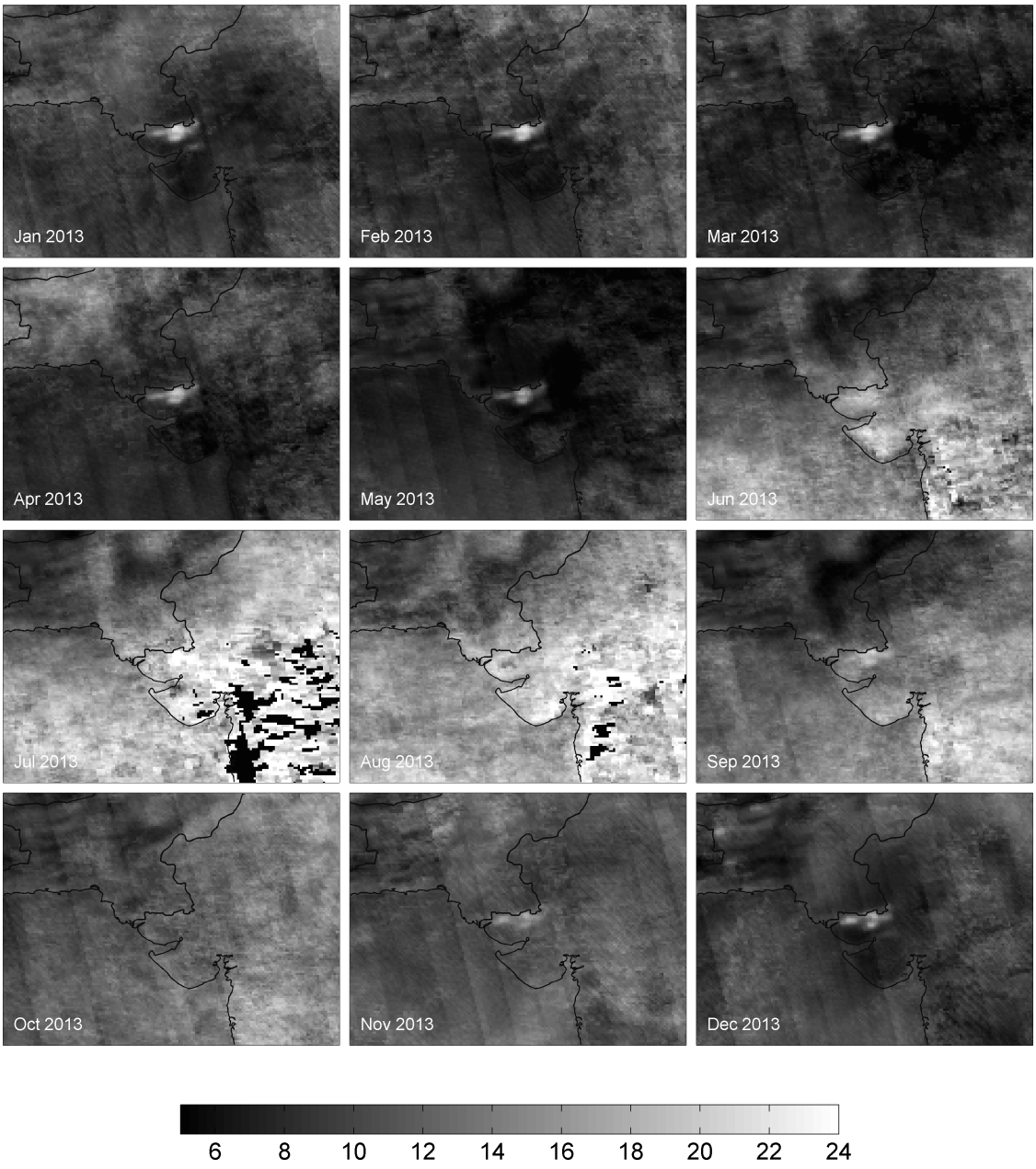

Figure 24. Seasonal variation of the monthly mean reflectivity at 331 nm over the Rann of Kutch as seen by OMI during 2013 (same data selection as in Figure 13, i.e. for CF<0.3).

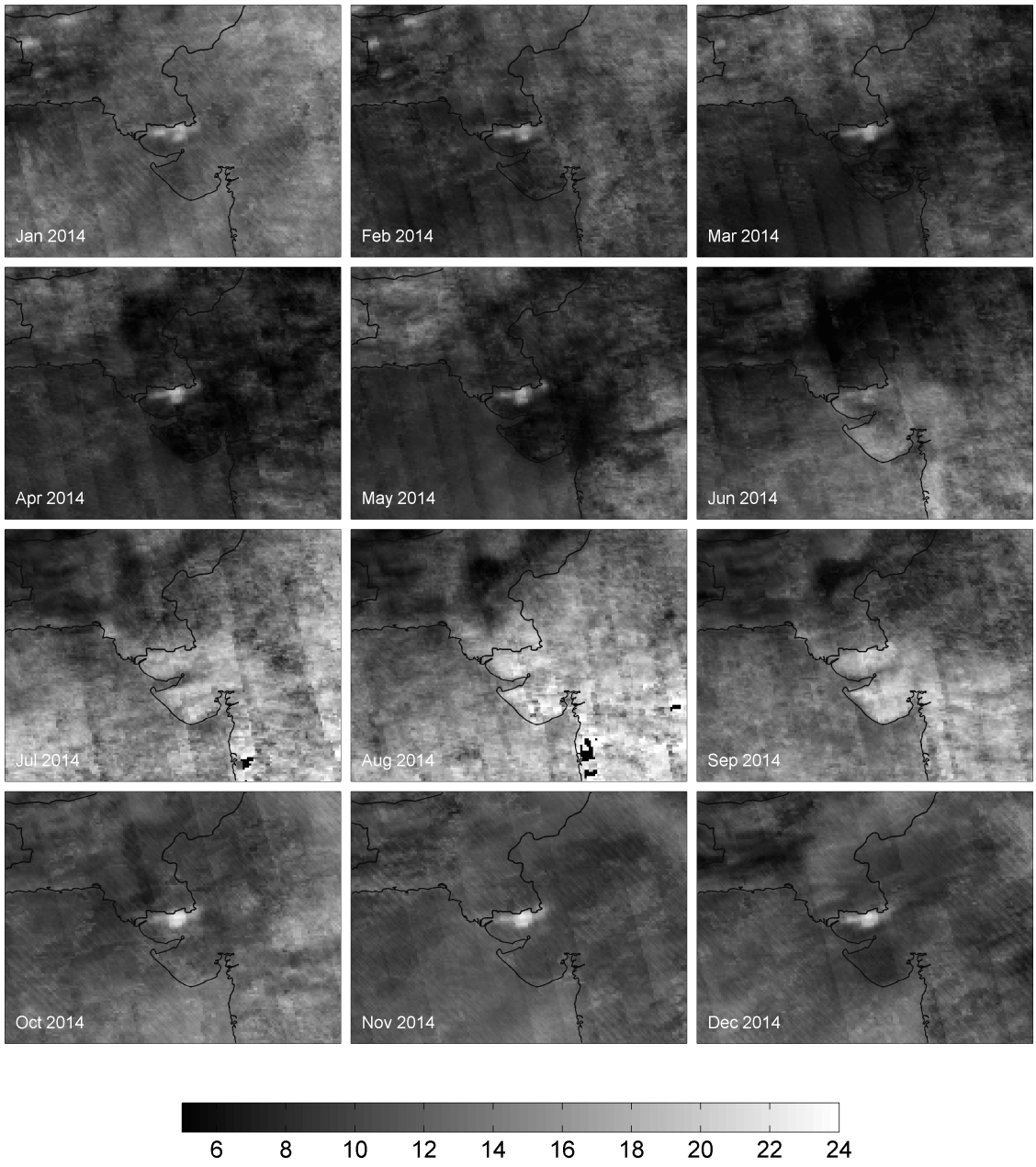

Figure 25. Seasonal variation of the monthly mean reflectivity at 331 nm over the Rann of Kutch as seen by OMI during 2014 (same data selection as in Figure 14, i.e. for CF<0.3).